

Electromagnetic dynamic stability analysis of power electronics-dominated systems using eigenstructure-preserved LTP Theory

Received: 9 October 2024

Accepted: 14 July 2025

Published online: 25 July 2025

 Check for updates

Jiabing Hu^{1,6}  , Zeren Guo^{1,6}  , Jianhang Zhu^{2,6}  , Jürgen Kurths³, Yunhe Hou², Buyang Du¹, Zefei Wu¹, Guojie Zhao¹, Yunfeng Liu⁴, Kai Xin⁴, Jianbo Guo⁵ & Shijie Cheng¹

Secure operation of power systems, one of the largest man-made systems, is crucial for economic development and societal well-being. Over the past century, initiatives like Europe's Super Grid and China's Dual Carbon plan have driven significant changes in power systems, leading to the widespread integration of diverse power electronic equipment. This has resulted in the emergence of power electronics-dominated power systems. However, they have experienced multiple electromagnetic oscillation accidents, causing large-scale renewable energy disconnections and even power equipment damage. To address these critical stability issues, now a global concern, the prevalent method relies on linear time-invariant approximate modeling, i.e., the eigenstructure-reconfiguration framework. While effective, it is limited by the curse of dimensionality in large-scale systems. Recently, the linear time-periodic theory has shown potential in accelerating calculations, but its analysis methods remain underdeveloped. In response to these challenges, we propose here a generalized linear time-periodic participation factor and sensitivity theory within the eigenstructure-preserved framework. This proposed participation factor significantly improves computational efficiency, outperforming eigenstructure-reconfiguration methods by orders of magnitude. Additionally, the proposed sensitivity analysis overcomes the lack of its analyticity. The potential of our methods is demonstrated through real-world power systems of China.

Maintaining stability following small perturbations is crucial for dynamic systems, necessitating reliance on linear stability analysis. This viewpoint is particularly relevant to power systems^{1–3}, where the quantitative analysis must adapt to the high-order characteristics: large-scale power systems often consist of hundreds of thousands of nodes, and the system states and parameters expand significantly.

Therefore, it is imperative to investigate both the stability itself and the correlation between stability and states or parameters. Traditional power systems, dominated by synchronous generators, face significant challenges associated with electromechanical dynamics^{4–10}. Here, the dynamics could be described by a nonlinear time-invariant (NLTI) model, where linearization is performed around equilibrium

¹State Key Laboratory of Advanced Electromagnetic Technology, School of Electrical and Electronic Engineering, Huazhong University of Science and Technology, Wuhan, China. ²Department of Electrical and Electronic Engineering, The University of Hong Kong, Hong Kong, SAR, China. ³Institute of Physics, Humboldt-University, Berlin, Germany. ⁴Huawei Technologies Co., Ltd, Shanghai, China. ⁵China Electric Power Research Institute, Beijing, China. ⁶These authors contributed equally: Jiabing Hu, Zeren Guo, Jianhang Zhu.  e-mail: j.hu@mail.hust.edu.cn; jianhang@hku.hk

points (i.e., constant value). Extensive research has been conducted on this linear stability, focusing on eigenvalues^{4,5}, participation factors^{6,7}, and sensitivities^{8,10}, all within the framework of the linear time-invariant (LTI) theory. Eigenvectors, which are fundamental to participation factors and sensitivities (see Methods), along with eigenvalues, form the LTI eigenstructure⁶—the foundation of electromechanical dynamics. Over the past few decades, their successful application has formed the theoretical basis for analyzing and optimizing the electromechanical stability of traditional power systems.

Recent developments in power systems, driven by initiatives such as Europe's Super Grid plan¹¹, the United States' Building a Better Grid Initiative¹², and China's Dual Carbon plan¹³, have significantly changed their system composition^{14,15}. The integration of diverse power electronic equipment, including solar photovoltaics (PV), wind power, and high-voltage direct current (HVDC) transmission, has become widespread. These changes have resulted in what are now referred to as power electronics-dominated power systems¹⁶ (PEPS). In China, the transformation of the power grid has accelerated rapidly. By 2023, the installed capacity of PV increased by 55.2% year-on-year to 610 million kilowatts, while wind power capacity rose by 20.7% to 440 million kilowatts. Consequently, the proportion of these renewable sources in total power generation capacity exceeded 36%¹⁷, with projections indicating it will reach 48% by 2030 and 75.5% by 2050^{18,19}. However, this rapid development of PEPS has raised increasing concerns about stability issues, particularly those associated with electromagnetic dynamics. The early adoption of renewable energy in the United States brought about initial challenges, such as sub-synchronous oscillation (SSO) accidents in doubly fed induction generator-based wind farms connected to series compensated networks in Minnesota (2007) and Texas (2009). These accidents resulted in large-scale turbine trips and damage to crowbar protection circuits^{20,21}. Similar issues emerged in China, where in 2010, hundreds of SSO accidents in Hebei Guyuan's wind farms led to the disconnection of thousands of wind turbines²². In 2015, an SSO accident in Xinjiang Hami involving direct-drive permanent magnetic synchronous generator-based wind farms first occurred²³, causing the tripping of several large-capacity synchronous generators located hundreds of kilometers away, triggering significant power shortages and system frequency drops. Subsequently, electromagnetic oscillation accidents occurred frequently in practical PEPS^{24–27}, having become a major concern and posing a significant threat to the safe and stable operation.

However, in the electromagnetic timescale, complex time-varying characteristics emerge in PEPS due to several phenomena, such as positive–negative sequence coupling in renewable power generation (RPG) and switching operations in HVDC systems (see Supplementary Notes 1 and 2). As a result, electromagnetic dynamics are here best described using nonlinear time-periodic (NLTP) models, where steady-state behaviors converge to diverse periodic orbits. These orbits are no longer limited to simple sinusoidal waveforms at a fundamental frequency; instead, they include rich harmonic content—such as second-order components inherent in RPG internal dynamics and modular multilevel converter-based HVDC submodules, as well as the $12k \pm 1$ characteristic harmonics typical of line-commutated converter (LCC)-based HVDC systems^{28–30}. Furthermore, unlike traditional electromechanical dynamics, the electromagnetic dynamics of PEPS exhibit more pronounced high-order characteristics. This is partly due to the relatively low capacity of individual RPG units, and PEPS often require hundreds of units to replace a single synchronous generator. Additionally, PEPS include a large number of states associated with inductance and capacitance at the electromagnetic timescale—factors typically neglected in electromechanical models. Consequently, electromagnetic oscillations in PEPS are fundamentally linked to the stability of periodic orbits in high-order NLTP systems, becoming a topic of growing interest across physics and engineering^{31–36}.

Many attempts have been made for the electromagnetic dynamic stability evaluation of PEPS. Currently, the most frequently used methods, which involve Park transformation³⁷, dynamic phasor (DP)³⁸, and harmonic state-space (HSS)³⁹, rely on approximately transforming linear time-periodic (LTP) eigenstructure into LTI eigenstructure (Supplementary Notes 3). We categorize these methods within the eigenstructure-reconfiguration (ER) theoretical framework. However, each of these methods has limitations. The Park transformation essentially multiplies system variables by a rotating exponential factor, which restricts its applicability to systems dominated by a single frequency component⁴⁰. Unlike traditional power systems, where the time-varying inductance matrix of synchronous generators can be simplified into time-invariant differential-algebraic equations³⁷, the multiple interacting frequencies in PEPS make such simplification infeasible—even under balanced grid conditions (see also Supplementary fig. 1). Similarly, while the DP method offers flexibility, it may fail to capture key dynamics, especially in common control scenarios like phase-locked loops (PLLs) involving nested trigonometric expressions. Moreover, HSS utilizes Fourier series and harmonic balance, resulting in the ER-LTI model's order being the multiplication of system orders, making it impractical for large-scale PEPS due to the curse of dimensionality⁴¹. In summary, time-invariant methods struggle to accurately represent the general time-varying behavior of NLTP systems, limiting the broader application of the ER framework in PEPS.

In recent surveys^{42,43}, linear stability analysis with preserved time-varying characteristics holds great potential, especially for large-scale systems. However, its related analysis methods are still immature. Therefore, we focus on the EP theoretical framework of LTP systems—inspired by the Floquet general solution⁴⁴, which allows for a qualitative analysis directly incorporating time-varying characteristics, as shown in Fig. 1. The EP framework avoids the additional transformation required in the ER framework. Despite its potential, the EP framework has seen limited development, as earlier research primarily addressed small-scale, low-order LTP systems, such as the Mathieu equation, which is fundamental in physics and has only second-order dynamics⁴⁵. In such cases, the Floquet theory alone is sufficient for stability assessment. In contrast, PEPS with high-order characteristics require new tools to analyze the interaction between stability and system states or parameters. To meet this need, we propose here a generalized LTP participation factor and sensitivity theory, establishing a direct correlation between eigenvalues and time-varying states or parameters. Meanwhile, the proposed LTP participation factor theory enables an accurate and highly efficient analysis (where the ER framework faces trade-offs) of the electromagnetic linear stability in large-scale PEPS. The proposed sensitivity analysis overcomes the lack of its analyticity. Furthermore, it reveals that traditional LTI stability analysis is a special case of our more general LTP theory. Our research can also be extended to dynamic stability analysis in diverse systems with periodic coefficients^{31–33}.

Analysis method of LTP systems with EP framework

Unlike LTI systems that focus on stability around a constant equilibrium point, LTP systems assess stability within the neighborhood of periodic orbits. For a stability analysis of linear systems, three key questions must be answered: Is the system stable? Which factors dominate its stability? How do system parameters influence stability? These questions are equally relevant for LTP systems. However, existing analytical methods for LTP systems remain underdeveloped, and only the first question has been solved by Floquet theory⁴⁴ (see Methods).

To answer the remaining questions, we propose corresponding analysis methods within the EP theoretical framework of LTP systems (Supplementary Notes 4 and Supplementary fig. 2). Answering these questions requires defining the eigenvectors of the LTP system, which are rarely involved. Here, we construct them through the

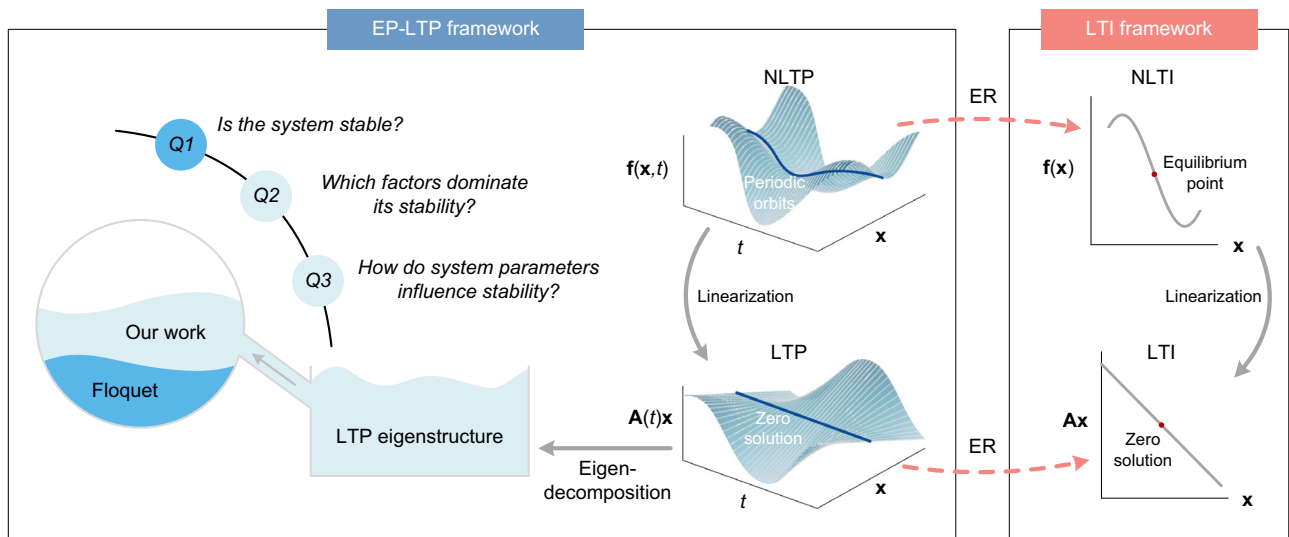


Fig. 1 | Overview of the EP-LTP framework and its connection to the LTI framework. Extensive research on the linear stability of NLTP systems has traditionally been conducted within the LTI framework using ER techniques. However, existing ER methods—such as the Park and DP methods, which convert NLTP systems into NLTI forms, and the HSS method, which approximates LTP systems as LTI forms—face significant challenges. In contrast, the EP-LTP framework aims to avoid

additional transformations and directly maintains the system’s original LTP eigenstructure for linear stability analysis, allowing modeling and analysis to be performed within the LTP framework. Nevertheless, stability analysis for LTP systems has traditionally relied solely on Floquet theory for assessing overall system stability. To address this, we further evaluate the correlation between stability and states or parameters through the LTP eigenstructure analysis.

diagonalization and invariance of the system matrix $A(t)$, achieved using a time-periodic matrix $R(t)$. Then, the column vector $r_k(t)$ in $R(t)$ and the row vector $l_k(t)$ in $L(t)=R^{-1}(t)$ denote the right and left eigenvectors corresponding to the eigenvalue λ_k , respectively (Supplementary Notes 4).

The correlation between modes and states, i.e., the participation factor, helps address the second key question. The key to correlation assessment lies in establishing a mapping mechanism. Previous interpretations^{46,47} based on state and mode energy concepts⁴⁸ have been limited to LTI systems. Hence, we generalize this energy-based interpretation when constructing the LTP system’s participation factor analysis method. Due to the energy summation invariance, the mapping relationship between state energy and mode energy can be expressed by the elements of $R(t)$ and $L(t)$ (Supplementary Notes 4). Therefore, we define the participation factor matrix P as $\{R(t) \odot L^T(t)\}_0$, where \odot denotes the Hadamard product, and $\{\}_0$ represents the mean or average value over a period.

The correlation between modes and parameters, i.e., sensitivity, addresses the third question, which can be treated through the gradient of modes to parameters. Unlike traditional approaches that focus solely on time-invariant parameters^{31–33}, we explore the significant influence of time-varying components. In real-world systems, this makes the modes functional in mathematics, not just functions of time-varying parameters. Thus, we derive the functional derivative of $\lambda_k[\alpha(t)]$ along a direction defined by $\varphi(t)$, yielding a time-independent value. Then, the sensitivity of a mode to the concerned parameter $\alpha(t)$ is given by $\{l_k(t)(\delta A(t)/\delta \alpha(t))_{\varphi(t)} r_k(t)\}_0$ (Supplementary Notes 4).

Moreover, when $A(t)$ and the parameters are time-invariant, the participation factor and sensitivity reduce to the forms consistent with those of traditional LTI systems (Supplementary Notes 4 and Supplementary fig. 2). Therefore, the analysis method for the LTI system (see Methods) can be regarded as a special case of the proposed LTP system analysis method.

Eigenstructure analysis

We apply the proposed EP-LTP analysis method in real PEPS of the Hami power grid in Northwest China, which is a typical nonlinear time-varying system with a large-scale RPG²⁸ and an LCC-HVDC²⁹. Besides,

the details of the utilized models are introduced in Supplementary Notes 2. To fairly compare the proposed EP-LTP analysis method against the traditional ER-LTI in electromagnetic dynamics stability analysis, we model the Hami power grid as a testing system. All tests are completed on a Dell Workstation, 52 CPUs with Intel (R) Gold 6230 R, 2.1 GHz.

The eigenvalues and eigenvectors analysis are the prerequisite for further participation factor and sensitivity analysis. We compare the proposed EP-LTP analysis method with a mature LTI model, which performs the best and is most commonly used in terms of accuracy, namely the HSS model³⁹. Besides, the drawbacks of the Park and DP methods are illustrated in detail in Supplementary Notes 3. The HSS model, based on Fourier series approximation and harmonic balance principles, relies on a critical parameter: the truncation number, which determines the maximum harmonic dynamics considered. This parameter is vital for maintaining the model’s accuracy⁴¹ and will be discussed in subsequent comparative studies.

To better summarize the quantitative relationship between the order of the small-signal model and computational efficiency, we constructed multiple testing systems (including 813th-order and 2263th-order testing systems), reflecting the dynamics of different power devices (Supplementary Notes 6). The overall comparative results for all testing systems are shown in Fig. 2a. The HSS model requires different truncation numbers for various stability issues, and we report the time costs of the eigenstructure analysis for five truncation numbers (i.e., 2, 4, 8, 16, and 29). For all testing systems, the EP-LTP method consistently has a shorter time cost compared to the HSS model. The time cost is proportional to the third-order polynomial of the model order n_c , which is suitable for both EP-LTP and ER-LTI. Therefore, as the system scale expands or the required truncation number increases, the advantages of the proposed EP-LTP method become more prominent. For the testing system of $n = 813$, the EP-LTP method is even 2000 times faster than traditional ER-LTI methods with a truncation number of 29, which ensures an accurate calculation of the eigenvalues with real parts > -0.8 . This real-part threshold is artificially set, and a smaller threshold would allow for a more comprehensive characterization of the electromagnetic dynamics in large-scale PEPS.

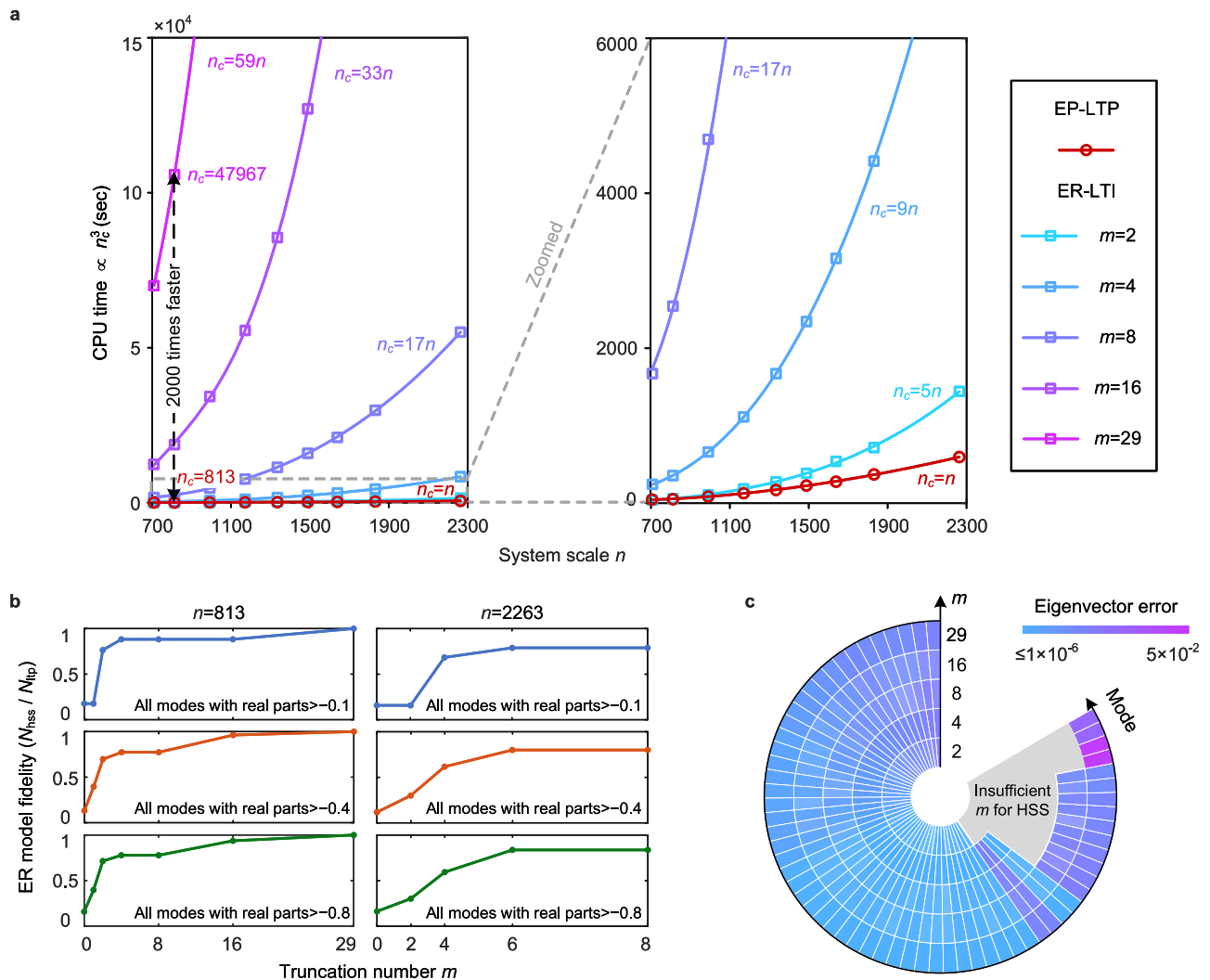


Fig. 2 | Comparison of efficiency and accuracy between EP-LTP and ER-LTI frameworks in eigenstructure calculations. **a** CPU time required to compute both eigenvalues and eigenvectors. Points of different shapes represent the EP-LTP model and the ER-LTI models with different truncation numbers m . A third-order polynomial fit (i.e., CPU time $< n^3$) is applied to capture the CPU time trend, where n_c denotes the model order. Specifically, $n_c = n$ for the EP-LTP model and $n_c = n(2m + 1)$ for the ER-LTI models, with n representing the system scale. Additional details are provided in the Supplementary Information. **b** ER-LTI model fidelity compared with EP-LTP model. Three specific damping ranges (i.e., the real parts of eigenvalues $\sigma > -0.1$, -0.4 , and -0.8 , the modes within these ranges are prone to instability) are focused on, represented as blue, red, and green lines,

respectively. Under different damping ranges, the eigenvalue number is N_{LTP} for the EP-LTP model. Besides, the accurate number of eigenvalues obtained by ER-LTI is N_{HSS} . We use the quotient of N_{HSS} and N_{LTP} to represent the fidelity of the HSS models in different damping ranges. **c** Eigenvector error between EP-LTP and ER-LTI. A comparison is performed in the 813th-order testing system, where a high truncation number guarantees the accuracy of all modes with real parts > -0.8 . The corresponding eigenvector results are consistent between the EP-LTP and ER-LTI models with the truncation number 29. See Supplementary Notes 6 for details and a quantitative interpretation of the accuracy indices. Source data are provided as a Source Data file.

To further demonstrate the advantages, we compare the eigenstructure accuracy through the 813th-order and 2263th-order testing systems. Based on the Floquet theory, the eigenvalues of the EP-LTP method are reliable within the range of numerical calculation accuracy. Therefore, Fig. 2b shows the accuracy rate between the ER-LTI eigenvalues with different truncation numbers and EP-LTP eigenvalues, considering only eigenvalues with real parts greater than σ ($\sigma = -0.1$, -0.4 , and -0.8). The accuracy improves with higher truncation numbers for the ER-LTI method, but EP-LTP maintains reliable accuracy with lower computational demands. Besides, based on Supplementary Notes 3, the Fourier coefficients of the EP-LTP eigenvectors are theoretically equivalent to the eigenvectors of the HSS model. Consequently, the accuracy of the ER-LTI eigenvectors still relies on the same truncation number required for eigenvalue accuracy (Fig. 2c). Since the ER-LTI method demands higher truncation numbers for accuracy,

it will result in exceptionally computationally expensive effort, showing the significant advantage of the proposed EP-LTP method.

Participation factor analysis

We apply the proposed eigenvectors to the EP-LTP participation factor analysis. Besides, the ER-LTI participation factor analysis results are taken as the comparison object, which comes from the HSS model and traditional LTI participation factor analysis methods. Since the ER-LTI participation factors characterize the contribution of Fourier coefficients of each state to each eigenvalue, synthesis processing is required (Supplementary Notes 4).

We take the 813th-order and 2263rd-order testing systems for comparative analysis. The time required to calculate the participation factors includes the time spent on both eigenstructure and participation factor calculations. As shown in Fig. 3a, although the proposed

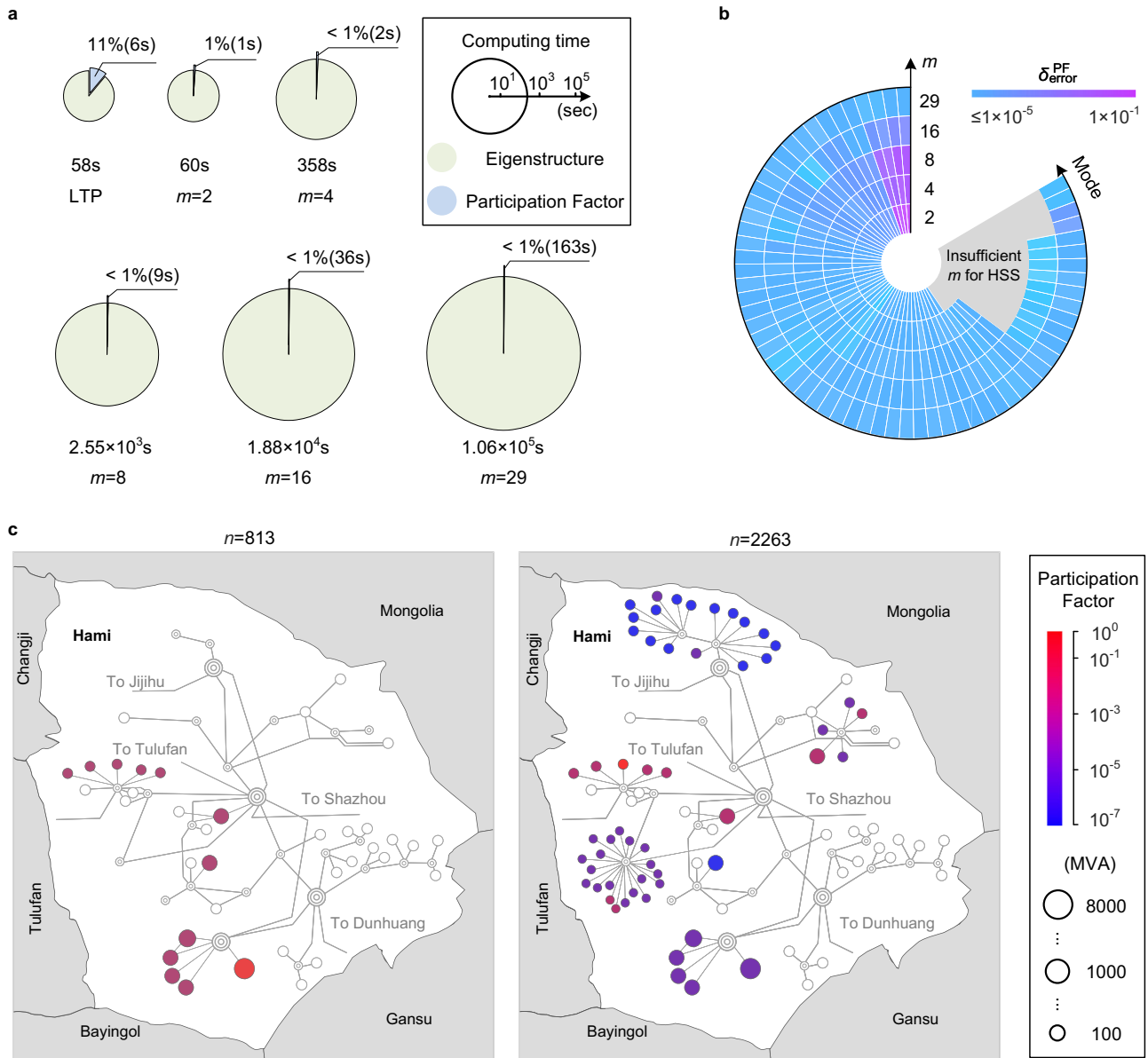


Fig. 3 | Comparison of efficiency and accuracy between EP-LTP and ER-LTI frameworks and visualization in participation factor computation. **a** CPU time required to compute the participation factor. The circle’s radius represents the sum of computing time for the eigenstructure and participation factors. The blue sector represents the proportion of the participation factor computing time. **b** Participation factor error between EP-LTP and ER-LTI. See Supplementary Notes 6 for details and a quantitative interpretation of the accuracy indices. **c** Hami power

grid structure and participation factor analysis. The participation factor of equipment is obtained by summarizing the participation factor of each state within the equipment⁵⁹. The color-coded circles denote the equipment whose participation factor is greater than 10^{-7} , with the color indicating the corresponding participation factor. The radius of the circle represents the capacity of different equipment. The concentric circles denote the substation. Source data are provided as a Source Data file.

LTP participation factors offer no significant advantage over the ER-LTI participation factors in the 813th-order testing system, there is a huge difference in the time cost for calculating the eigenstructure (see Supplementary Table 1). Since the eigenstructure calculation is essential for a participation factor analysis, the proposed LTP method overall demonstrates a significant efficiency advantage. Then, the participation factor error between ER-LTI and EP-LTP is shown in Fig.3b, where only eigenvalues with the real parts greater than -0.8 are considered (Supplementary Notes 6 defines participation factor error). As the truncation number increases, the participation factor error decreases (see Supplementary Table 2 for comparison results of all testing systems). To ensure an accurate participation factor analysis

for all eigenvalues, the ER-LTI method requires a truncation number greater than 29, significantly increasing computation time.

For the weaker damping modes of concern of both testing systems, the dominant units based on the LTP participation factors are given in Fig. 3c. In the 813th-order testing system, the dominant units include RPG and LCC-HVDC. The necessity of a larger truncation number (i.e., here is larger than 29) for ER-LTI, due to LCC-HVDC participation, highlights why standard LCC-HVDC models⁴⁹ from IEEE working groups often fail to capture key electromagnetic stability issues (also see Supplementary fig. 4). In contrast, in the 2263th-order testing system, where the dominant units are only RPG, a lower truncation number can meet the requirements for an accurate analysis.

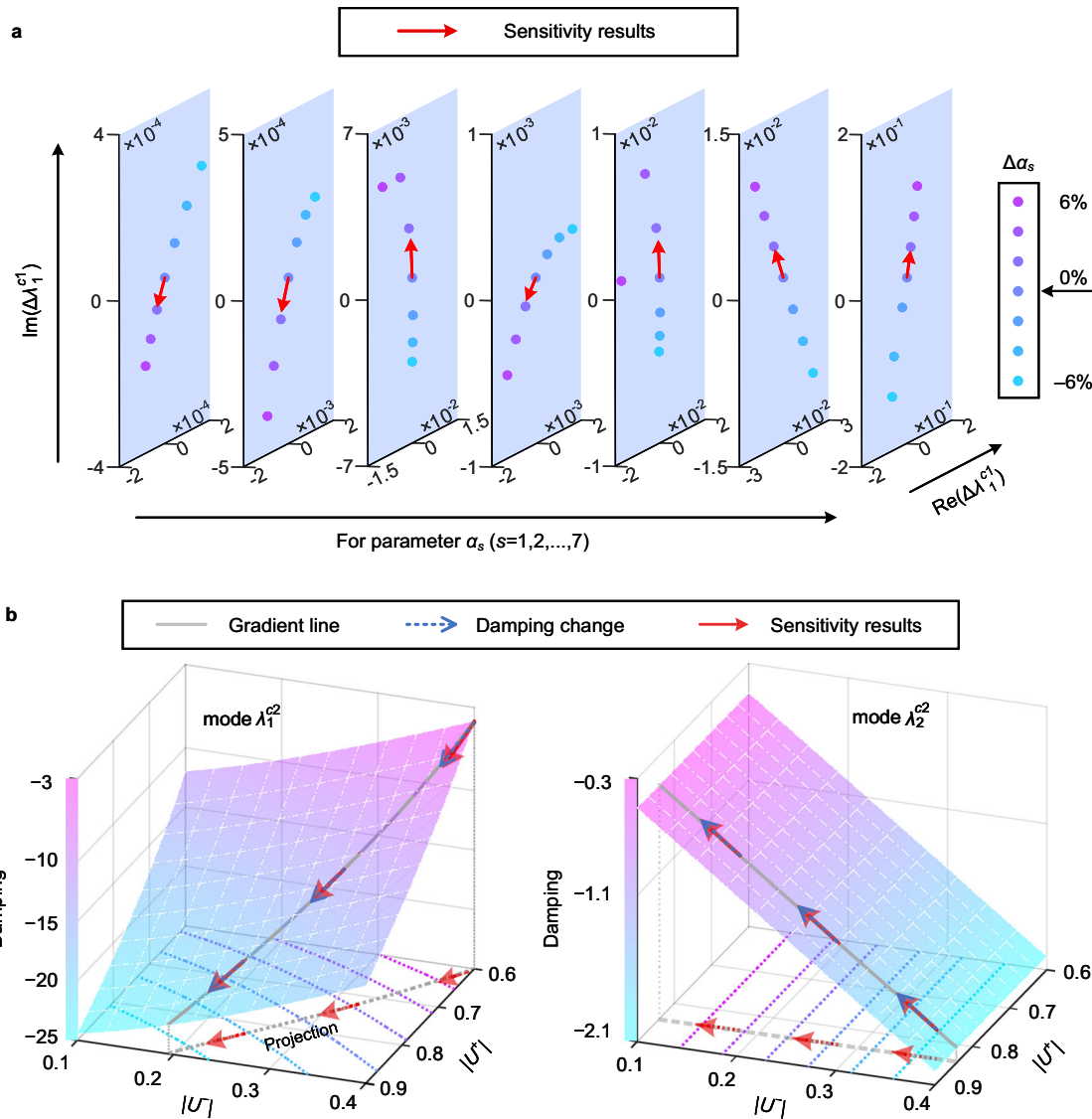


Fig. 4 | EP-LTP framework is accurate in sensitivity analysis. **a** Case 1: to time-invariant control parameters of the dominant equipment. The color-coded circles represent the practical change of the concern mode λ_1^{c1} , with the color indicating the parameter variation from -6% to 6%. Sensitivity analysis is performed based on a common point (0%), also marked as the origin of all red arrows. With the parameter variation of 2%, the sensitivity analytical results (end of red arrows) closely approximate the eigenvalue changes. **b** Case 2: to time-varying voltage vector $\mathbf{u}^s(t)$

of Jijihu station. Here, the variation form⁶⁰ of $\mathbf{u}^s(t)$ is $e^{j\omega t}$ and $e^{j\omega t}$. The intersection of the white dashed lines denotes the two concerned modes (i.e., λ_1^{c2} and λ_2^{c2}) with the different voltage conditions of Jijihu station. Two gradient lines (gray solid lines) are marked based on the fitted surfaces. With a variation of 1/30 along the gradient direction, the sensitivity analytical results (red solid arrows) accurately capture the damping changes (blue dashed arrows). Supplementary Notes 6 provides more details. Source data are provided as a Source Data file.

Sensitivity analysis

In large-scale PEPS, thousands of system parameters influence electromagnetic dynamic stability. For the influence of system parameters on linear stability, due to the lack of sensitivity analyticity, the traditional method mainly relies on the eigenvalue locus under the studied parameter range, which is commonly used in both the LTP model and the reasonably truncated HSS model. However, the traditional sensitivity analysis, which essentially involves traversing parameters, lacks a global understanding of system parameters and has poor efficiency. Here, the proposed EP-LTP sensitivity analysis method offers a more efficient way to assess the impact of massive system parameters on linear stability. Since sensitivity describes the change along the tangential direction of the eigenvalue locus, we use the eigenvalue locus to evaluate the correctness of the proposed LTP sensitivity analysis method.

Unlike LTI systems that only contain time-invariant parameters, LTP system parameters can generally be divided into two categories: time-invariant and periodic time-varying. For the time-invariant system parameters, the sensitivity analysis involves a function calculation. As shown in Fig. 4a, the impact of various control parameters on dominant eigenvalues is depicted. The eigenvalues motion trend from the sensitivity analysis is consistent with the actual eigenvalue motion. For the periodic time-varying system parameters, sensitivity analysis is more complex and involves functional calculations. Here, we examine the sensitivity of a time-varying voltage vector under unbalanced voltage conditions of power sources, reflecting real-world engineering scenarios. As shown in Fig. 4b, the impact of positive and negative sequence voltages on system stability varies. For the mode λ_1^{c2} , reducing the negative sequence voltage or increasing the positive sequence voltage will improve mode damping. However, for the mode λ_2^{c2} ,

increasing the negative sequence voltage will improve mode damping. The trends in system damping observed through LTP sensitivity analysis match the actual system damping variations. Therefore, the proposed LTP sensitivity analysis can successfully be applied to time-varying and time-invariant system parameters.

Results and discussion

In this paper, we present numerical calculation analysis methods for electromagnetic dynamic stability of large-scale PEPS within the eigenstructure-preserved linear time-periodic (EP-LTP) framework, which go substantially beyond existing EP-LTP approaches that only answer whether the system is stable. Our significant contributions include the development of the EP-LTP participation factor and sensitivity analysis methods, which answer the critical questions: which factors dominate system stability, and how parameters affect system eigenvalues. By comparing large-scale Hami PEPS in China, the proposed EP-LTP method produces more accurate results and lower computational costs in dominant factors analysis than the best-performing linear modeling and analysis methods in the eigenstructure-reconfiguration linear time-invariant (ER-LTI) framework, which are better suitable for small-scale systems. In this paper, the EP-LTP method can be more than 2000 times faster than the ER-LTI method. It should be noted that the multiplication amplification of small-signal model order in the ER-LTI framework is the intuitive reason for its computationally expensive effort. For the last question, the proposed EP-LTP method overcomes the lack of its analyticity, offers detailed insights into the influence of parameters on linear stability, and avoids the poor efficiency in traditional traversal methods, such as the eigenvalues locus. The generalizability of the proposed approach enables its direct application to other practical PEPSs, such as the 44–58 Hz oscillation event recorded in the Zhangbei project in China from 2020 to 2022^{50,51} (Supplementary fig. 3). This system integrates large-scale wind and solar generation with modular multilevel converter-based HVDC technology, representing a model for future power systems that rely entirely on power electronic devices. Furthermore, the analysis method of the LTI system is theoretically a special case of the proposed method.

However, the proposed method still faces two main challenges. The first is the growing need for real-time online analysis of the electromagnetic dynamics in large-scale PEPS. While the EP method significantly enhances both accuracy and computational efficiency compared to the widely used ER approach under typical hardware conditions, real-time analysis remains a substantial challenge and does not yet meet the operational requirements of power systems. Specifically, existing standards for electromechanical dynamics require rolling calculations to be completed within 15 minutes⁵², a timeframe that would need to be significantly shorter to accommodate the faster timescales of electromagnetic phenomena. Thus, further research into advanced numerical algorithms is essential to make real-time applications of the proposed method feasible. The second challenge involves the control of electromagnetic dynamic stability in PEPS. Beyond fast computation, effectively damping and suppressing electromagnetic oscillations is crucial to ensuring system reliability⁵³. While the proposed LTP-based participation and sensitivity analysis provide a strong theoretical basis for identifying optimal controller locations and tuning parameters, further work is needed to translate these insights into practical control strategies and develop effective stabilizers for electromagnetic oscillations.

Although our methods were developed for electromagnetic dynamic stability analysis in PEPS, the underlying framework is broadly applicable. This generality stems from the fact that periodicity is a fundamental and elegant principle in nature, and many physical and engineering systems evolve under its influence. For instance, periodic behavior underlies the dynamics of accelerator operation, flow around circular cylinders, or aircraft design processes^{31,34–36}. As long as the

system's behavior can be modeled as the linear stability of NLTP systems or the dynamic stability of LTP systems, the proposed EP-LTP framework can be effectively applied for stability analysis. Looking to the future, we anticipate that as research shifts from small-scale to large-scale periodic systems, the LTP theory will find increasing relevance in a broad range of domains, such as biological systems⁵⁴ and chemical systems⁵⁵, supporting their stable operation and further development.

Methods

Linearization

The concept of linear stability addresses the dynamics near the steady-state of nonlinear systems, whose nonlinearity is described by

$$\dot{\mathbf{y}}(t) = \mathbf{f}(t; \mathbf{y}(t)) \quad (1)$$

where the vector $\mathbf{y}(t) = [y_1(t), y_2(t), \dots, y_n(t)]^T$ describes the n states at time t , $\mathbf{f} = [f_1, f_2, \dots, f_n]^T$ denotes the vector field.

The steady-state form $\mathbf{y}_{ss}(t)$ satisfies $\dot{\mathbf{y}}_{ss}(t) = \mathbf{f}(t; \mathbf{y}_{ss}(t))$. Applying Lyapunov's first method, the dynamics of the disturbance $\mathbf{x}(t) = \mathbf{y}(t) - \mathbf{y}_{ss}(t)$ can be expressed as

$$\dot{\mathbf{x}}(t) = \dot{\mathbf{y}}(t) - \dot{\mathbf{y}}_{ss}(t) = \left. \frac{\partial \mathbf{f}}{\partial \mathbf{y}} \right|_{\mathbf{y}_{ss}(t)} \mathbf{x}(t) + o(\mathbf{x}(t)) \quad (2)$$

where $o(\mathbf{x}(t))$ denotes higher-order infinitesimals and is neglected in the linearized system; $\partial \mathbf{f} / \partial \mathbf{y}$ is the Jacobian matrix of \mathbf{f} concerning states \mathbf{y} .

When the steady-state form is a periodic orbit (i.e., $\mathbf{y}_{ss}(t) = \mathbf{y}_{ss}(t + T)$, and T is the period), the linear stability is determined by LTP systems, when \mathbf{y}_{ss} is a special periodic orbit, such as a constant value or equilibrium point, LTI systems determine the linear stability.

LTI eigenstructure

With the constant state matrix \mathbf{A} , $\dot{\mathbf{x}}(t) = \mathbf{A}\mathbf{x}(t)$ represents the LTI systems. Assuming that \mathbf{A} has n distinct (acceptable in most real-world systems) eigenvalues $\{\lambda_k, k = 1, 2, \dots, n\}$, the eigenvalue matrix could be represented as $\mathbf{\Lambda} = \mathbf{R}^{-1}\mathbf{A}\mathbf{R} = \text{diag}(\lambda_1, \lambda_2, \dots, \lambda_n)$. The time-invariant matrices \mathbf{R} and $\mathbf{L} = \mathbf{R}^{-1}$ are the right and left eigenvector matrices. Furthermore, \mathbf{r}_k in $\mathbf{R} = [\mathbf{r}_1, \mathbf{r}_2, \dots, \mathbf{r}_n]$ and \mathbf{l}_k in $\mathbf{L} = [\mathbf{l}_1, \mathbf{l}_2, \dots, \mathbf{l}_n]$ denote the right and left eigenvectors corresponding to the eigenvalue λ_k . The eigenvalue and eigenvector calculations are performed using MATLAB.

LTI participation factor

The time-invariant eigenvectors form the decoupled coordinate transformation between states and modes. Various perspectives have been proposed to evaluate the correlation between modes and states, yet they predominantly lead to a unified form of the participation factor matrix, that is $\mathbf{P} = \mathbf{R}\mathbf{O}\mathbf{L}^T$ (Supplementary Notes 4). This formula exclusively incorporates the information of eigenvectors, thus enabling direct derivation of the participation factors after calculating the LTI eigenstructure.

LTI sensitivity

LTI sensitivity⁸ establishes the correlation between modes and parameters in LTI systems, which is derived as $\partial \lambda_k / \partial \alpha = \mathbf{l}_k^T (\partial \mathbf{A} / \partial \alpha) \mathbf{r}_k$. Apart from the eigenvectors, it requires the partial derivative of the state matrix with respect to the parameter α . In nonlinear dynamic systems, the state matrix is the function of steady states and parameters¹⁰, i.e., $\mathbf{A}(\mathbf{y}_{ss}, \alpha)$.

Therefore, there are two pathways through which α influences \mathbf{A} : a direct path, denoted by \mathbf{A}_E , where α is explicitly incorporated into \mathbf{A} , and an indirect path, denoted by \mathbf{A}_I , where α is implicitly incorporated

into \mathbf{A} . Considering these two pathways, $\partial \mathbf{A}(\mathbf{y}_{ss}, \alpha) / \partial \alpha$ is

$$\frac{\partial \mathbf{A}(\mathbf{y}_{ss}, \alpha)}{\partial \alpha} = \frac{\partial \mathbf{A}_E}{\partial \alpha} + \frac{\partial \mathbf{A}_I}{\partial \mathbf{y}} \bigg|_{\mathbf{y}_{ss}} \frac{\partial \mathbf{y}_{ss}}{\partial \alpha} \quad (3)$$

where both $\partial \mathbf{A}_E / \partial \alpha$ and $\partial \mathbf{A}_I / \partial \mathbf{y}$ could be derived using the Symbolic Math Toolbox of MATLAB⁵⁶. In the case where the steady-state form represents an equilibrium point, the partial derivative of the equilibrium points \mathbf{y}_{ss} concerning the parameter α is described by

$$\frac{\partial \mathbf{y}_{ss}}{\partial \alpha} = -\mathbf{A}^{-1} \frac{\partial \mathbf{f}}{\partial \alpha} \bigg|_{\mathbf{y}_{ss}} \quad (4)$$

Applying these procedures to LTI systems enables the computation of sensitivities.

LTP eigenvalue calculation

The general solution of Floquet theory is not analytical; therefore, numerical computation is required to obtain the LTP eigenvalues. First, the linear systems' state transition matrix (STM) satisfies

$$\dot{\Phi}(t, 0) = \mathbf{A}(t)\Phi(t, 0) \quad (5)$$

where $\Phi(t, 0)$ could map the states value from $\mathbf{x}(0)$ to $\mathbf{x}(t)$, that is $\mathbf{x}(t) = \Phi(t, 0)\mathbf{x}(0)$.

Based on the Floquet theory, we have $\Phi(t, 0) = \mathbf{P}(t)e^{\mathbf{Q}t}$ for LTP systems. With the boundary conditions $\mathbf{P}(0) = \mathbf{P}(T) = \mathbf{I}$ (\mathbf{I} denotes the identity matrix), the time-invariant matrix \mathbf{Q} is related to the STM $\Phi(T, 0)$ (i.e., $\Phi(T, 0) = e^{\mathbf{Q}T}$). Hence, how to obtain the $\Phi(T, 0)$ is the focus of the Floquet theory-based LTP eigenvalue calculation. Here, we apply the discrete exponential expansion method⁵⁷, where $\Phi(T, 0)$ is divided into the product of a series of STM.

$$\Phi(T, 0) = \prod_{K=1}^{N_d} \Phi(K\Delta t, (K-1)\Delta t) \quad (6)$$

Within each interval (i.e., $(K-1)\Delta t - K\Delta t$, $\Delta t = T/N_d$, N_d represents the number of intervals), the variation of the state matrix $\mathbf{A}(t)$ is neglected, and the STM of this interval could be calculated by

$$\Phi(K\Delta t, (K-1)\Delta t) = e^{\mathbf{A}(t_{K-1})\Delta t}, t_{K-1} = (K-1)\Delta t \quad (7)$$

The matrix exponential replaces numerical integration to accelerate the calculation process. The accuracy could be ensured by appropriately selecting N_d . Parallel computation could further accelerate the matrix exponential calculation at various time intervals. The matrix \mathbf{Q} is then calculated by $\ln[\Phi(T, 0)]/T$. The eigenstructure decomposition of \mathbf{Q} eventually leads to the LTP eigenvalues.

Choice of computational language

The proposed method was implemented in MATLAB, chosen for its robust support for matrix-based computations and its widespread use within the power systems research community. For the stability analysis, we utilized MATLAB's Symbolic Math Toolbox and Linear Algebra Toolbox. The functions in the Linear Algebra Toolbox are built on optimized LAPACK routines, ensuring high computational efficiency and numerical accuracy. In addition, the system model was structured to allow for easy data export and direct application of LAPACK-based tools if needed.

Data availability

The source data underlying Figs. 2–4, and Supplementary Fig. 4 are available at Figshare⁵⁸. The authors declare that the data supporting the findings of this study are available within the supplementary information files and Figshare. Source data are provided with this paper.

Code availability

The codes that support the findings of this study are available at Figshare⁵⁸.

References

- Kundur, P., Balu, N. J. & Lauby, M. G. *Power system stability and control*, 7 (McGraw-Hill, New York, 1994)
- Machowski, J., Bialek, J. W. & Bumby, J. R. *Power system dynamics: stability and control* (Wiley, 2008).
- Menck, P. J., Heitzig, J., Marwan, N. & Kurths, J. How basin stability complements the linear-stability paradigm. *Nat. Phys.* **9**, 89–92 (2013).
- Motter, A. E., Myers, S. A., Anghel, M. & Nishikawa, T. Spontaneous synchrony in power-grid networks. *Nat. Phys.* **9**, 191–197 (2013).
- Wong, D. Y. et al. Eigenvalue analysis of very large power systems. *IEEE Trans. Power Syst.* **3**, 472–480 (1988).
- Vergheze, G. C., Perez-Arriaga, I. J. & Schweppe, F. C. Selective modal analysis with applications to electric power systems, part II: the dynamic stability problem. *IEEE Trans. Power Appl. Syst.* **101**, 3126–3134 (1982).
- Hassan, L. H. et al. Optimization of power system stabilizers using participation factor and genetic algorithm. *Int. J. Electr. Power Energy Syst.* **55**, 668–679 (2014).
- Van, N. essJ., Boyle, J. & Imad, F. Sensitivities of large, multiple-loop control systems. *IEEE Trans. Autom. Control.* **10**, 308–315 (1965).
- Witthaut, D. et al. Collective nonlinear dynamics and self-organization in decentralized power grids. *Rev. Mod. Phys.* **94**, 015005 (2022).
- Wang, K. W., Chung, C. Y. & Tse, C. T. Multimachine eigenvalue sensitivities of power system parameters. *IEEE Trans. Power Syst.* **15**, 741–747 (2000).
- Macilwain, C. Energy: super grid. *Nature* **468**, 624–625 (2010).
- Department of Energy. Building a better grid initiative. <https://www.energy.gov/oe/articles/building-better-grid-initiative>. (2022).
- Mallapaty, S. How China could be carbon neutral by mid-century. *Nature* **586**, 482–484 (2020).
- Schäfer, B. et al. Non-Gaussian power grid frequency fluctuations characterized by Lévy-stable laws and superstatistics. *Nat. Energy* **3**, 119–126 (2018).
- Sajadi, A., Kenyon, R. W. & Hodge, B. M. Synchronization in electric power networks with inherent heterogeneity up to 100% inverter-based renewable generation. *Nat. Commun.* **13**, 2490 (2022).
- Yuan, X., Hu, J. & Cheng, S. Multi-time scale dynamics in power electronics-dominated power systems. *Front. Mech. Eng.* **12**, 303–311 (2017).
- Statistical data of China's power industry 2023 (National Energy Administration). https://www.nea.gov.cn/2024-01/26/c_1310762246.htm. 2023
- Global Energy Interconnection Development and Cooperation Organization (GEIDCO). Research Reports on China's CO2 Emission Peak and Carbon Neutrality Released in Beijing. <https://en.geidco.org.cn/2021/0322/3277.shtml> (2021).
- Wang, Y. et al. Accelerating the energy transition towards photovoltaic and wind in China. *Nature* **619**, 761–767 (2023).
- Mulawarman, A., Mysore, P. Detection of undamped sub-synchronous oscillations of wind generators with series compensated lines. *Minnesota Power Systems Conference*. 1–5 (2011).
- Irwin, G. D., Jindal, A. K., & Isaacs, A. L. Sub-synchronous control interactions between type 3 wind turbines and series compensated AC transmission systems. *IEEE Power & Energy Society General Meeting*, 1–6 (2011).
- Wang, L. et al. Investigation of SSR in Practical DFIG-Based Wind Farms Connected to a Series-Compensated Power System. *IEEE Trans. Power Syst.* **30**, 2772–2779 (2015).

23. Liu, H. et al. Sub-synchronous interaction between direct-drive PMSG based wind farms and weak AC networks. *IEEE Trans. Power Syst.* **32**, 4708–4720 (2017).
24. Wang, X. & Blaabjerg, F. Harmonic stability in power electronic-based power systems: Concept, modeling, and analysis. *IEEE Trans. Smart Grid* **10**, 2858–2870 (2018).
25. Chi, Y. et al. Overview of mechanism and mitigation measures on multi-frequency oscillation caused by large-scale integration of wind power. *CSEE J. Power Energy Syst.* **5**, 433–443 (2019).
26. Shair, J., Li, H., Hu, J. & Xie, X. Power system stability issues, classifications and research prospects in the context of high-penetration of renewables and power electronics. *Renew. Sustain. Energy Rev.* **145**, 111111 (2021).
27. Zou, C. et al. Analysis of resonance between a VSC-HVDC converter and the AC grid. *IEEE Trans. Power Electron.* **33**, 10157–10168 (2018).
28. Guan, L., Yao, J., Liu, R., Sun, P. & Gou, S. Small-signal stability analysis and enhanced control strategy for VSC system during weak-grid asymmetric faults. *IEEE Trans. Sustain. Energy* **12**, 2074–2085 (2021).
29. Du, B. et al. Small-signal modeling of LCC-HVDC considering switching dynamics based on the Linear Time-Periodic (LTP) method. *IEEE Trans. Power Del.* **39**, 2715–2728 (2024).
30. Zhu, J., Hu, J., Wang, S. & Wan, M. Small-signal modeling and analysis of MMC under unbalanced grid conditions based on linear time-periodic (LTP) method. *IEEE Trans. Power Del.* **36**, 205–214 (2021).
31. Giannetti, F., Camarri, S. & Citro, V. Sensitivity analysis and passive control of the secondary instability in the wake of a cylinder. *J. Fluid Mech.* **864**, 45–72 (2019).
32. Lasagna, D. Sensitivity analysis of chaotic systems using unstable periodic orbits. *SIAM J. Appl. Dyn. Syst.* **17**, 547–580 (2018).
33. Tamer, A. & Masarati, P. Generalized quantitative stability analysis of time-dependent comprehensive rotorcraft systems. *Aerospace* **9**, 10 (2021).
34. England, R. et al. Dielectric laser accelerators. *Rev. Mod. Phys.* **86**, 1337–1389 (2014).
35. Wang, J., Li, R. & Peng, X. Survey of nonlinear vibration of gear transmission systems. *Appl. Mech. Rev.* **56**, 309–329 (2003).
36. Lopez, M. & Prasad, J. Linear time invariant approximations of linear time periodic systems. *J. Am. Helicopter Soc.* **62**, 1–10 (2016).
37. Park, R. H. Two-reaction theory of synchronous machines generalized method of analysis-part I. *Trans. Am. Inst. Electr. Eng.* **48**, 716–727 (1929).
38. Sanders, S. R., Noworolski, J. M., Liu, X. Z. & Verghese, G. C. Generalized averaging method for power conversion circuits. *IEEE Trans. Power Electron.* **6**, 251–259 (1991).
39. Wereley, N. M. Analysis and control of linear periodically time-varying systems. Ph.D. dissertation, Department of Aeronautics and Astronautics, MIT, 217–223 (1991).
40. O'Rourke, C. J., Qasim, M. M., Overlin, M. R. & Kirtley, J. L. A Geometric interpretation of reference frames and transformations: dq0, Clarke, and Park. *IEEE Trans. Energy Convers.* **34**, 2070–2083 (2019).
41. Zhu, J. et al. Truncation number selection of the harmonic state-space model based on the Floquet characteristic exponent. *IEEE Trans. Ind. Electron.* **70**, 3222–3228 (2022).
42. Li, H. et al. A time-domain stability analysis method for grid-connected inverters with PR control based on Floquet theory. *IEEE Trans. Ind. Electron.* **68**, 11125–11134 (2020).
43. Golestan, S. et al. LTP modeling and stability assessment of multiple second-order generalized integrator-based signal processing/synchronization algorithms and their close variants. *IEEE Trans. Power Electron.* **37**, 5062–5077 (2021).
44. D'Angelo, H. Linear time-varying systems: analysis and synthesis. Boston, MA, USA: Allyn and Bacon (1970).
45. McLachlan, N. W. *Theory and Application of Mathieu Functions*. (Oxford University, New York, 1964).
46. Hamdan, A. M. A. Coupling measures between modes and state variables in power-system dynamics. *Int. J. Control* **43**, 1029–1041 (1986).
47. Iskakov, A. B. Definition of state-in-mode participation factors for modal analysis of linear systems. *IEEE Trans. Autom. Control* **66**, 5385–5392 (2021).
48. MacFarlane, A. G. J. Use of power and energy concepts in the analysis of multivariable feedback controllers. *Proc. Inst. Electr. Eng.* **116**, 1449–1452 (1969).
49. Szechtman, M., Wess, T., & Thio, C. V. A benchmark model for HVDC system studies. *IET ACDC*. 374–378 (1991).
50. Li, H. Z., Shair, J., Zhang, J. Q. & Xie, X. R. Investigation of sub-synchronous oscillation in a DFIG-based wind power plant connected to MTDC grid. *IEEE Trans. Power Syst.* **38**, 3222–3231 (2023).
51. Zheng, S. et al. Engineering data analysis of sub/super-synchronous oscillation between wind farm and MMC in Zhangbei project. In *IEEE 6th Conference on Energy Internet and Energy System Integration (EI2)*, 11–13 (2022).
52. Savulescu, S. C. *Real-time stability assessment in modern power system control centers*. (Wiley-IEEE, 2009).
53. Demello, F. P. & Concordia, C. Concepts of synchronous machine stability as affected by excitation control. *IEEE Trans. Power Appl. Syst.* **88**, 316–329 (1969).
54. Ushio, M. et al. Fluctuating interaction network and time-varying stability of a natural fish community. *Nature* **554**, 360–363 (2018).
55. Van Laake, L., Lüscher, T. & Young, M. The circadian clock in cardiovascular regulation and disease: lessons from the Nobel Prize in Physiology or Medicine 2017. *Eur. Heart J.* **39**, 2326–2329 (2018).
56. Lynch, S. *Dynamical systems with applications using MATLAB* (Birkhäuser, Boston, 2004).
57. Friedmann, P., Hammond, C. E. & Woo, T. H. Efficient numerical treatment of periodic systems with application to stability problems. *Int. J. Numer. Methods Eng.* **11**, 1117–1136 (1977).
58. Hu, J. et al. Datasets for electromagnetic dynamic stability analysis of power electronics-dominated systems using eigenstructure-preserved LTP theory. Figshare <https://doi.org/10.6084/m9.figshare.29064380>
59. Shuai, Z. et al. Parameter stability region analysis of islanded microgrid based on bifurcation theory. *IEEE Trans. Smart Grid* **10**, 6580–6591 (2019).
60. Harnefors, L. Modeling of three-phase dynamic systems using complex transfer functions and transfer matrices. *IEEE Trans. Ind. Electron.* **54**, 2239–2248 (2007).

Acknowledgements

J.H., Z.G., J.Z., B.D., Z.W., and G.Z. were supported by the National Science Foundation of China under Grant 52225704, Grant U22B20122, and Grant 52107196. Y.H. and J.Z. were supported in part by the Theme-based Research Scheme from the Research Grants Council, Hong Kong SAR, under Grant T23-713/22-R, and in part by Collaborative Research Fund from the Research Grants Council, Hong Kong SAR, under Grant C1052-21GF. Besides, we gratefully acknowledge master's student Jiali Kui for their assistance with data analysis and information collection.

Author contributions

J.H., Z.G., and J.Z. conceived the idea, led the project, conducted the theoretical analysis, and wrote the initial manuscript and revisions. J.K. and Y.H. contributed ideas and methods for the theoretical analysis and participated in the writing of the paper. B.D., Z.W., G.Z., Y.L., and K.X. also conducted a theoretical analysis and contributed to the manuscript. J.G. and S.C. provided guidance to all co-authors throughout the process.

Competing interests

The authors declare no competing interests.

Additional information

Supplementary information The online version contains supplementary material available at <https://doi.org/10.1038/s41467-025-62183-1>.

Correspondence and requests for materials should be addressed to Jiabing Hu or Jianhang Zhu.

Peer review information *Nature Communications* thanks Juri Belikov, Rodrigo Henriquez-Auba and the other, anonymous, reviewer(s) for their contribution to the peer review of this work. A peer review file is available.

Reprints and permissions information is available at <http://www.nature.com/reprints>

Publisher's note Springer Nature remains neutral with regard to jurisdictional claims in published maps and institutional affiliations.

Open Access This article is licensed under a Creative Commons Attribution-NonCommercial-NoDerivatives 4.0 International License, which permits any non-commercial use, sharing, distribution and reproduction in any medium or format, as long as you give appropriate credit to the original author(s) and the source, provide a link to the Creative Commons licence, and indicate if you modified the licensed material. You do not have permission under this licence to share adapted material derived from this article or parts of it. The images or other third party material in this article are included in the article's Creative Commons licence, unless indicated otherwise in a credit line to the material. If material is not included in the article's Creative Commons licence and your intended use is not permitted by statutory regulation or exceeds the permitted use, you will need to obtain permission directly from the copyright holder. To view a copy of this licence, visit <http://creativecommons.org/licenses/by-nc-nd/4.0/>.

© The Author(s) 2025